Engineering Science and Technology, an International Journal 43 (2023) 101440

HOSTED BY

Contents lists available at ScienceDirect

Engineering Science and Technology, an International Journal

journal homepage: www.elsevier.com/locate/jestch

Highly selective multiple-notched UWB-MIMO antenna with low correlation using an innovative parasitic decoupling structure

Anees Abbas [a], Niamat Hussain [b], Md Abu Sufian [a], Wahaj Abbas Awan [a], Jinkyu Jung [a], Sang Min Lee [c], Nam Kim [a,*]

[a] Department of Information and Communication, Chungbuk National University, Cheongju 28644, Republic of Korea
[b] Department of Smart Device Engineering, Sejong University, Seoul 05006, Republic of Korea
[c] Department of Corporate Support Centre, Korea National University of Transportation, Chungju 27469, Republic of Korea

ARTICLE INFO

Article history:
Received 27 December 2022
Revised 10 May 2023
Accepted 15 May 2023
Available online 31 May 2023

Keywords:
Ultrawide Band
Antenna
Multi–inputmultioutput antenna
Electromagnetic bandgap
Decoupling structure

ABSTRACT

In ultra-wideband (UWB) communications, highly selective notch bands are required to avoid interference with other licensed bands. This study presents a highly selective triple-notch UWB-MIMO antenna, which consists of a four-radiating patch antenna and an isolator. The single-element antenna consists of a radiating patch, substrate, ground plane, electromagnetic bandgap (EBG) structures, and split ring resonators (SRR). To achieve the designated UWB bandwidth, the lower edges of the antenna patch are cut by a quarter-circle radius. The three sharp notches are achieved by utilizing four EBGs and two SRRs at the back of the antenna. The notch bandwidth can also be controlled by changing the parameters such as the width and length of the EBG structure and SRR. The single antenna is then translated into 4-port MIMO systems. The high correlation between elements is reduced by inserting a unique parasitic decoupling structure. The decoupling structure is designed in a way that reduces the mutual coupling in all passbands. The proposed antenna offers a ($|S_{11}| < -10$ dB) of 3.1 – 11.8 GHz impedance bandwidth. The proposed MIMO antenna having an overall size of $54 \times 54 \times 1.52$ mm3 is fabricated to verify the simulation results. The MIMO antenna shows exceptional diversity properties, including better isolation between unit elements of MIMO antenna (>20 dB), a diversity gain (DG) very close to 10 dB (>9.99 dB), an envelope correlation coefficient which is less than 0.001, and suitable mean effective gain is also in the defined range. The suggested parasitic element UWB – MIMO antenna thus supports its suitability for use in UWB communication networks.

1. Introduction

The ultra-wideband (UWB) radio protocol is a fast, safe, and reduced power that has gained the interest of academia and industry due to its befitting features like a high data transfer capacity, low power usage, cheap cost, and precise positioning and localization [1–9]. This band's (3.1–10.6 GHz) significance can be seen in advanced communication like target sensor collecting data, monitoring applications, precision locating, and even cell phones. However, nearby narrow frequency bands such as the 5 G mid-band spectrum (3.4–3.8 GHz), Wireless LAN band (5.15–5.825 GHz), and ITU satellite downlink communication (7.25–7.75 GHz) interfere with the UWB band. In antenna design, the concept of notch bands involves creating a resonant circuit that is tuned to a specific frequency that needs to be attenuated. The EBGS and SRRs were used to create the filtering characteristics in the conventional notch bands. The central frequencies of these stop bands are brought together to realize highly selective notch bands. Various filtering antennas with different approaches have been devised to overcome the interference caused by the aforementioned bands and have been published in the literature [10–15]. In the literature, single and multiple band-notched antennas have been published to prevent interference. These antennas are designed with various techniques, such as cutting slots in the radiating patch, EBG/SRR structures, and filter structures in the ground plane or antenna feed in traditional UWB technology, reflection and diffraction are always problems with the medium, resulting in multipath fading and causing signal losses resulting in poor end-to-end communication..

* Corresponding author.
E-mail addresses: anees@chungbuk.ac.kr (A. Abbas), niamathussain@sejong.ac.kr (N. Hussain), sufian@chungbuk.ac.kr (M.A. Sufian), wahajabbasawan@chungbuk.ac.kr (W.A. Awan), yoona106@chungbuk.ac.kr (J. Jung), leesm@ut.ac.kr (S.M. Lee), namkim@chungbuk.ac.kr (N. Kim).

https://doi.org/10.1016/j.jestch.2023.101440
2215-0986/

The MIMO technology is then used as a solution in communication systems to provide minimal multipath fading and improve transmission quality. MIMO antenna systems are used in wireless communication to improve the capacity and reliability of wireless links by using multiple antennas at both ends of the communication system. The basic principle of the MIMO system is to allow multiple independent streams by more than one antenna as shown in Fig. 1. The researchers have applied different techniques to improve the capacity of the MIMO channel. In [16], three conventional notch bands have been achieved by using EBG structures in the UWB MIMO antenna. While a 10-element MIMO antenna that works at sub-6 GHz bands and LTE bands is proposed without providing any solution to avoid interference from other licensed bands [17]. Moreover, different shapes of parasitic decoupling structures [18–25], decoupling networks [26], defected ground systems [27], neutralization lines [28], slotted stub [29], metamaterials [30–32] and the metasurface [33–34].

A quad port UWB–MIMO antenna is proposed [23], where a fan-shaped decoupling structure is used on the top side of the substrate to reduce mutual coupling. The decoupling network technique is utilized in the proposed antenna [26] to enhance the performance of the quad port MIMO system. Moreover, the mutual coupling is reduced in the antenna [27] without using any decoupling structure. At the same time, the presented antenna [28–29] applied neutralization lines and slotted stubs to enhance the mutual coupling for performance improvement of MIMO antennas, respectively. Furthermore, the performance of the MIMO antenna [22] is improved by Mesh-Like decoupling structure, in [33–34] isolation is enhanced using metasurface, a unique substance that does not occur in nature and can control electromagnetic waves. In the proposed antenna [34], metasurface and slot structures are designed efficiently on the ground plane for two bands to improve isolation and decrease mutual coupling. Both decoupling methods effectively improve antenna isolation, the metamaterials are applied for the lower range frequencies while the slots are applied to the higher band.

The main purpose of this study is to develop a MIMO antenna for UWB technology that offers optimized data speed and increases the radio link's capacity for transmission by simultaneously offering numerous signal routes. To boost the signal-to-noise ratio and error rate, several copies of the same signal must be created. This gives the data more chances to reach the receiving antenna unaffected by fading. Additionally, limits any interference from the already existing bands very sharply within the UWB spectrum, such as 5G sub-6 GHz, WLAN band, and satellite downlink band by applying a novel parasitic decoupling structure.

However, we have proposed an antenna with sharp notch bands (high selective), which almost equally stops interference from the lower frequency to the highest frequency of the notch bands. The high selective notch band attenuates or suppresses a specific range of frequencies while allowing all other frequencies to pass through unaffected. In this antenna, the high selectivity of the notch band has been achieved by merging two different conventional notched bands. In the [13], our previous published work has only a single stop band at the WLAN band, and not offering a MIMO system. While this research paper presents a 4-port UWB–MIMO antenna operating at 3.1–11.8 GHz, which covers the whole UWB bandwidth with three sharp stop bands. The lower 5G and WLAN band selective notch characteristic is determined by two pairs of EBGs, and the satellite downlink band is achieved by applying a pair of SRRs. The notch band of the antenna can also be modified when required just by changing the width and lengths of EBGs and the SRRs. Moreover, a novel decoupling structure is incorporated in the center of the MIMO antenna to decrease the effect of electromagnetic interaction among unit elements. The proposed decoupling structure is useful, and the presented UWB-MIMO antenna satisfies the requirements of MIMO systems by offering high isolation, very low ECC, and good diversity gain.

2. UWB-MIMO design procedure

2.1. Single element

The zig-zag pattern flat antenna has the benefits of compactness, small size, lightweight, and ease of processing. However, the length of the patch will have an impact on the resonance properties of the antenna during the design process. The current path will be extended as the length increases, which will cause the resonance frequency to change to a low frequency. The formula for calculating the antenna length is given in Eq. (1) [35].

$$L = c/4f\sqrt{\varepsilon}r \tag{1}$$

In this equation, L is the antenna's length, f is its resonance frequency, and c is the rate at which electromagnetic waves travel in a medium. To determine the UWB frequency band's lower band-edge frequency (f1) for monopole antennas Eq. (2) [36] is used.

$$f_1 = \frac{7 \cdot 2}{(l + \gamma + P) \times k} \tag{2}$$

Where p is the distance between the ground plane and the radiator, while the l is length, and r is the width of the monopole radiator.

The design of the single-element antenna starts with a 16 × 12 mm2 radiating patch, then the lower ends are truncated with a half-semi-circle to achieve UWB bandwidth. The antenna consists of the radiating patch, ground plan, four electromagnetic bandgap structures (EBG), and pair of split-ring resonators (SRR). These copper elements are printed on the front and back of Taconic TLY 5 lossy substrates having a thickness of 1.52 mm, ε_r = 2.2, and

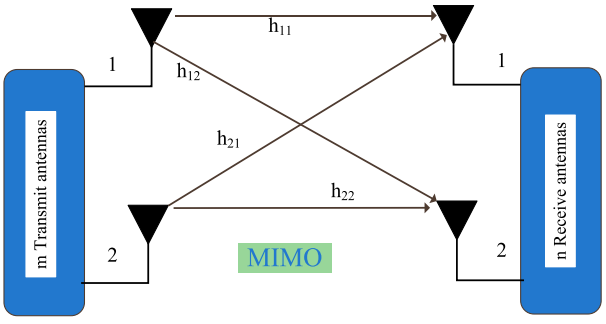

Fig. 1. The basic representation of the MIMO antenna system.

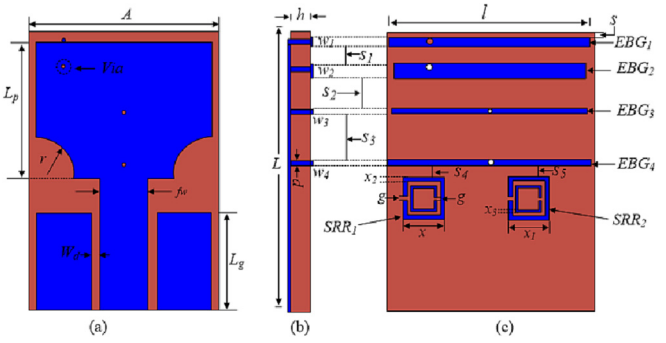

Fig. 2. The geometry of the unit-element of the proposed UWB-MIMO antenna (a) front view (b) side view and (c) back side of the antenna.

tanδ = 0.0009. The antenna geometry is shown in Fig. 2, while Table 1 displays the optimized parameters for the single-element antenna.

The UWB bandwidth is accomplished by subtracting the lower corners of the patch with a half semi-circle. The sub-6 5G band and WLAN band are notched by introducing different lengths of EBGs while the satellite downlink band interference is stopped by incorporating two SRRs. The $|S_{11}|$ the sharp triple-notched UWB antennas are shown in Fig. 3. The notching characteristics at 5G sub-6 GHz and WLAN bands controlled by two pairs of EBG structures. The parameters (l, w, *and* $_s$) of the rectangular EBG structures are tuned to acquire a quasi-rectangular notch band by combining two traditional notched bands. Similarly, a highly selective notch at the satellite downlink band is achieved by adjusting the length of the SRRs.

The realized gain of the single-element antenna is shown in Fig. 4. The antenna shows stable gain (2–4.6 dBi) characteristics at the operating frequencies. While it reduced up to a low level of −4.5 dBi at the notched bands, verifying the excellent notching ability of the antenna.

The antenna's ability to convert electrical power into electromagnetic waves is often indicated by its radiation efficiency and shown in Fig. 5. It can be seen that the antenna offers a high radiation efficiency of>93% in the entire frequency range of interest. However, in the notch bands it sharply decreased as low as 50%.

2.2. Parametric study of notch controllability

The antenna also has the advantage of adjusting the notch bands following the requirements. The parameters of the EBG structures and SRRs can be altered as needed to change the notch bands. As an example, by changing the parameter of EBG3-4 the WLAN band notch is extended from 5.25 to 5.75 GHz to 5–6 GHz to prove the idea as shown in Fig. 6.

The increment in the size of EBGs shifts a notch to lower frequencies, however, due to the compactness of the antenna, the length of EBGs cannot be increased further. Therefore, the position of the shorting pins used in shifting the notch to lower frequencies can be seen in EBG1-2 as the position of vias ai changed to acquire the notch of the 5 G Sub-6 GHz band. The change in dimensions of EBGs also affects other notch bands so we have to readjust the parameters of SRR parameters as well. Table 2 displays the parameters of the UWB antenna.

2.3. Design of the proposed MIMO antenna

In radio communication, MIMO is a technique for increasing a radio link's capacity by employing multiple transmission and receiving antennas to take advantage of multipath propagation. The maximum quantity of data that can be sent via any channel or medium is determined by the Shannon capacity theorem given in Equation (3) and can be applied to determine the capacity of a MIMO antenna.

$$C_{MIMO} \approx m(BW\text{Log}2(1+\text{SNR})) = \text{m}C_{SISO} \quad (3)$$

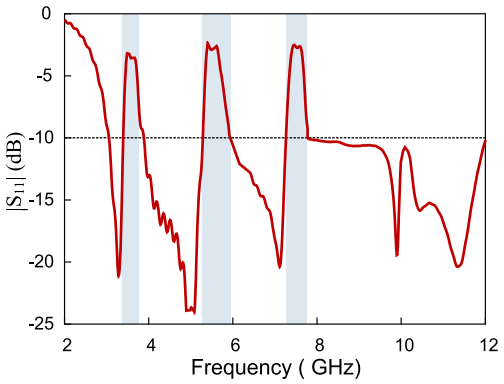

Fig. 3. The antenna's $|S_{11}|$ characteristics with triple spectrum rejection.

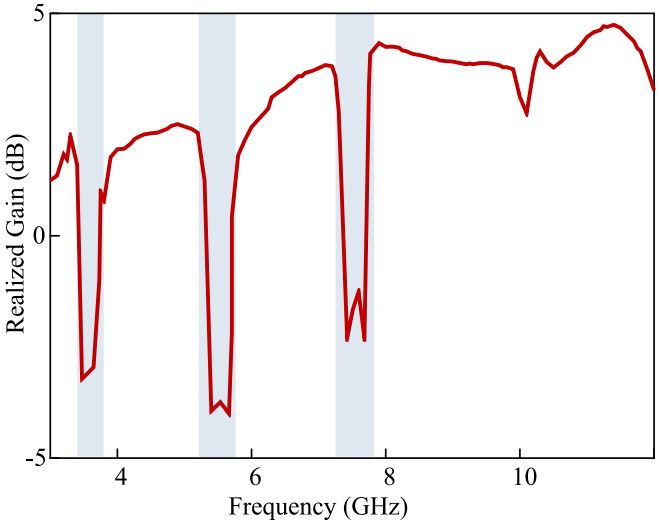

Fig. 4. The realized gain of the single element antenna.

In the above equation, C represents capacity, and m represents the number of antennas, which is increased m times without additional power or bandwidth.

The design is an extension of the single-element antenna to the MIMO antenna system. The initial stage of the 4-port MIMO system is depicted in Fig. 7a, which is constructed by placing four single elements orthogonally without any sort of decoupling mechanism between them. The space between the vertical antenna is kept at 14 mm while the distance between diagonal antennas is 20 mm. To keep the compactness of the MIMO antenna possible minimum distance is kept assured. The S-parameter of the MIMO antenna is depicted in Fig. 7b. From the figures, the performance of MIMO shows that antennas are closely coupled which affects the radiation performance of each element, especially in lower and higher frequencies. To overcome the mutual coupling a parasitic decoupling structure is introduced to provide unaffected radiation performance of the MIMO system.

Table 1
Optimized parameters of the single-element antenna (unit = mm).

Par	Val.	Par	Val.	Par	Val.	Par	Val.
a	20	lp	12	l1	18.25	w2	1.25
l	26	wp	16	l2	17.25	w3	0.4
h	1.52	r	3.6	l3	17.5	w4	0.4
lg	8.8	fw	4.4	l4	18.4	x	3.7
wg	5.15	wd	0.65	w1	0.8	x1	3.8

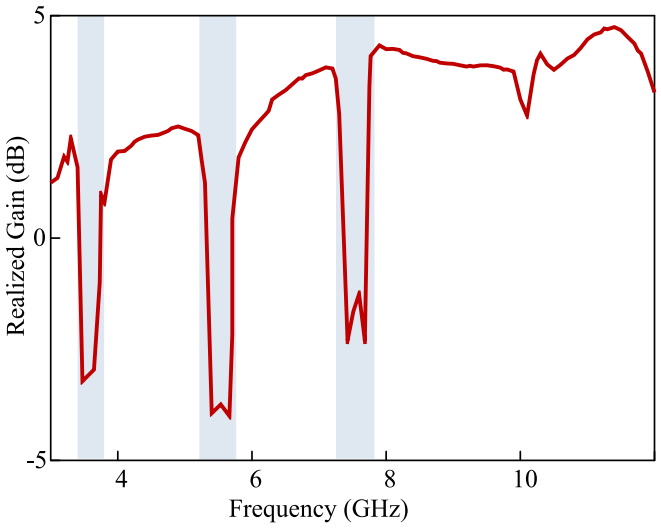

Fig. 5. The radiation efficiency of the single-element antenna.

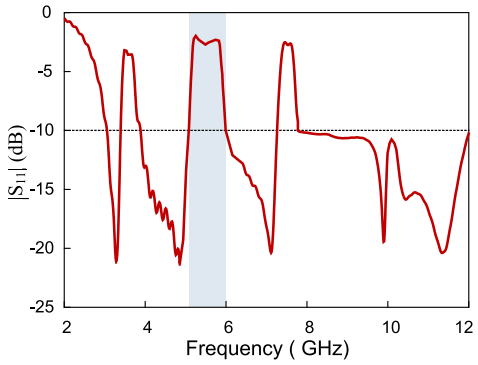

Fig. 6. Extended notch band by controlling the parameters of EBG3 and EBG4.

2.4. Design stages of decoupling structure

The idea behind multiplicity is to send the same signals in multiple paths to receivers. It significantly lowers signal loss and enhances link performance. This is accomplished by time diversity, in which the same message is broadcast at various periods. Even so, designing a MIMO antenna without any degradation of single-element performance is challenging. The multi-radiating elements closely arranged together cause an increase in the mutual coupling and high correlation in the channel, which lessens the performance of MIMO systems. The mutual coupling degrades the signal-to-interference noise ratio (SINR) of the MIMO elements. This decreases the performance of the MIMO antenna [35]. To encounter this issue, researchers have used different techniques such as parasitic elements [22], decoupling networks [26], defected ground structure [27], neutralization lines [28], metamaterials [32], and metasurface [33–34].

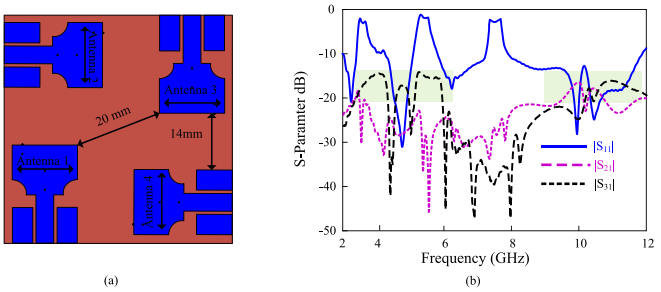

Fig. 7. UWB-MIMO antenna without isolation technique (a) antenna geometry and (b) S-parameter results.

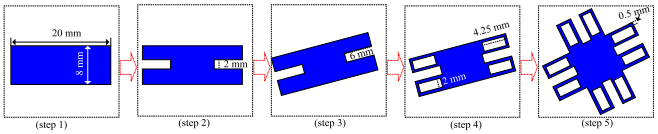

Fig. 8. The design stages of the proposed decoupling structure.

An innovative parasitic decoupling structure in this MIMO antenna is designed to minimize the reciprocal coupling of coexisting elements. Initially, at step 1 rectangular parasitic patches of length, 20 mm and 8 mm width are designed in the center of the MIMO antenna system. The parasitic patch's center is then sliced at both ends with 2 × 6 mm cuts at step 2 and rotated 22 degrees at step 3. Furthermore, four 2 × 4.5 mm slots are etched onto the ends of the H-shaped decoupler at step 4. Moreover, the parasitic decoupler is rotated at 90 degrees and copied, then both structures are added in final step 5. The proposed parasitic decoupling structure's design stages are depicted in Fig. 8.

In step 3, the structure is rotated at 22 degrees because its length is the same as the diagonal separation between radiating elements. Thus, it affects the antenna's reflection coefficient. The response of the transmission coefficient at various phases of the decoupling structure can be seen in Fig. 9a and 9b. The decoupling structure shows the best response at stage 5. For a clear understanding of the response of decoupling structure diagonally (S13) and vertically (S12) between the antenna elements shown separately. The small-sized rectangles of parasitic decoupling structures reduce the electromagnetic interaction between the antenna elements at higher frequencies, while the central major part increases the correlation at lower frequencies.

To demonstrate the proposed decoupling structure's functionality, of the proposed UWB-MIMO antenna shown in Fig. 10, the surface current behavior at 4.5 GHz, 6.5 GHz, 8.5 GHz, and 11.5 GHz are depicted in Fig. 11 to express the validity of decoupling structure. Due to the electromagnetic behavior of the radiating elements, when only one element of the MIMO antenna is excited, the current is induced in the other elements which causes mutual coupling. This creates an impact on the MIMO antenna's overall performance. To reduce the corresponding consequences, we proposed the decoupling structure. The induced current is discontin-

Table 2
Optimized parameters of the proposed MIMO antenna (unit = mm).

Par	Val.	Par	Val.	Par	Val.	Par	Val.
a	20	lp	12	l1	18.25	w2	1.25
l	26	wp	16	l2	17.25	w3	0.4
h	1.52	r	3.6	l3	17.7	w4	0.4
lg	8.8	fw	4.4	l4	18.8	x	3.7
wg	5.15	wd	0.65	w1	0.8	x1	3.8

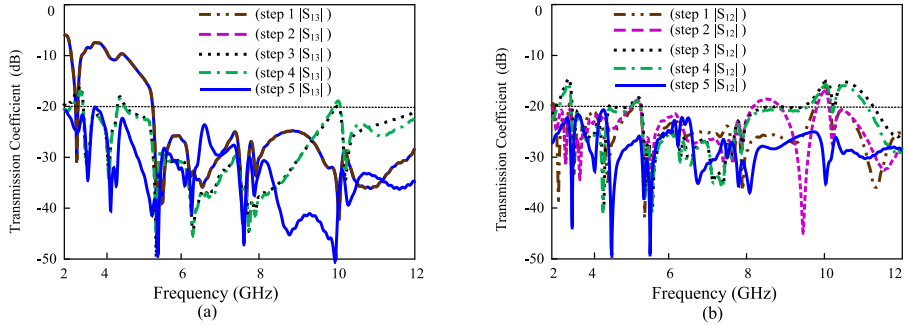

Fig. 9. Transmission coefficient at different stages of parasitic decoupling structure (a) $|S_{13}|$, (b) $|S_{12}|$.

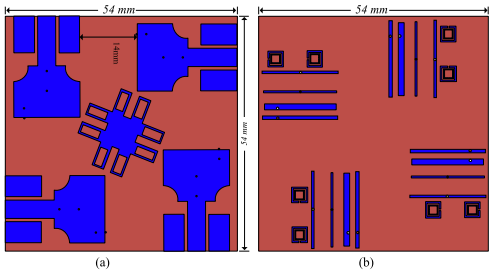

Fig. 10. The proposed UWB-MIMO antenna (a) frontside view (b) backside view.

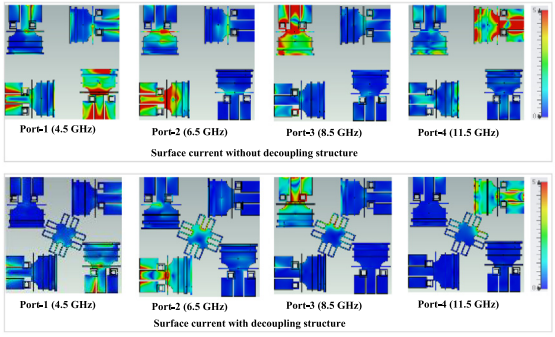

Fig. 11. The surface current of different ports at different frequencies with and without decoupling structure.

ued when the proposed decoupling structure is added, allowing the antenna to operate normally.

2.5. The parametric study of the decoupling structure

To give a clear idea about the robustness37–38 of the decoupling structure, we have made a parametric study of the decoupling structure, as shown in Fig. 10. The size of the proposed novel decoupling structure has been made smaller, and its results are compared with the proposed decoupling structure. The decoupling structure is designed in different sizes, and the proposed structure with 20 mm offers the best possible result for isolation. The structure was checked with a reduced size of up to 12 mm, as after this size the structure doesn't show any improvement in mutual coupling reduction. A comparison in terms of transmission coefficient results for both proposed and smaller-size decoupling structures are shown in Fig. 12. Due to symmetric design, the transmission coefficient's response is the same diagonally ($|S_{13}|$, $|S_{24}|$, $|S_{31}|$, $|S_{42}|$) and vertically ($|S_{12}|$, $|S_{21}|$, $|S_{14}|$, $|S_{41}|$, $|S_{23}|$, $|S_{32}|$, $|S_{43}|$, and $|S_{34}|$). Therefore, to avoid complexity only ($|S_{13}|$ and $|S_{12}|$) are shown in Fig. 13.

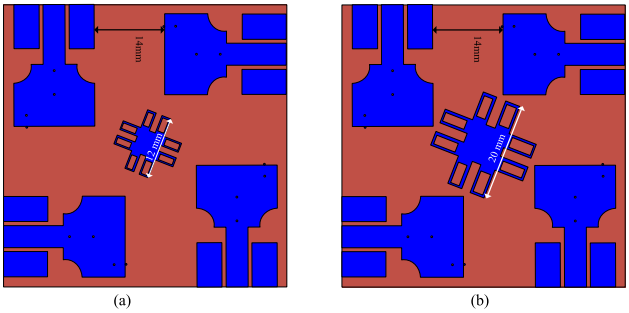

Fig. 12. The UWB-MIMO antenna with different size decoupling structures (a) 12 mm, and (b) 20 mm.

2.6. MIMO antenna performance comparison with and without proposed decoupling structure

The MIMO antenna results particularly the transmission coefficients are shown to demonstrate the validity of the proposed decoupling structures. Due to symmetric design, the transmission coefficient's response is the same diagonally ($|S_{13}|$, $|S_{24}|$, $|S_{31}|$, $|S_{42}|$) and vertically ($|S_{12}|$, $|S_{21}|$, $|S_{14}|$, $|S_{41}|$, $|S_{23}|$, $|S_{32}|$, $|S_{43}|$, and $|S_{34}|$). Therefore, to avoid complexity only ($|S_{13}|$ and $|S_{12}|$) are shown in Fig. 14. From the figure, it can be seen that the proposed decoupler has reduced the correlation between the antenna elements effectively.

3. Measured results and discussion

For experimental verification, the proposed antenna is imprinted on substrate Taconic TLY 5 lossy (thickness = 1.52 mm) (εr = 2.2 and tan = 0.0009), as shown in Fig. 15. An Agilent vector network was used to measure the planned antenna's impedance and radiation patterns. A well-calibrated standard horn antenna was used as the source antenna for the far-field test, and the fabricated sample was measured as the receiving antenna. Amplifiers are utilized both during transmission and reception to offer a consistent power reception. The measurement setup of the antenna is shown in Fig. 16. To find the values of gains at various orientations, the suggested manufactured antenna was rotated. Except for the notched band, the entire UWB band (3–11.8 GHz) exhibits good impedance matching. Table 3 displays the simulated and measured antenna element gains at 4.5 GHz, 6.5 GHz, 8.5 GHz, and 11.5 GHz while the radiation patterns for port-1 of different frequencies are presented in Fig. 17. During the test, only one port of the MIMO

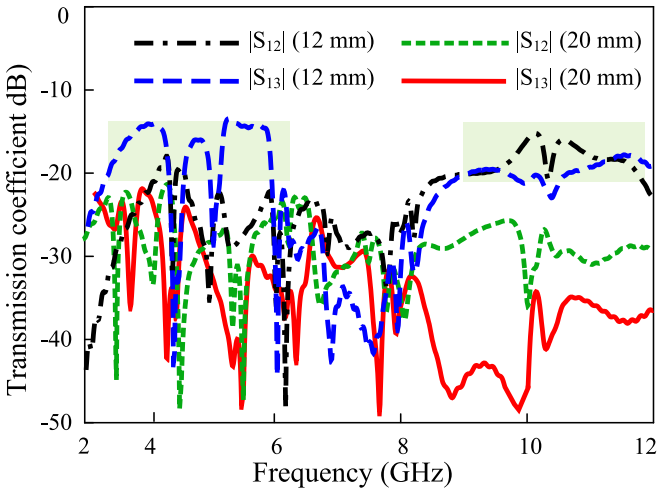

Fig. 13. The comparison of the transmission coefficient of UWB-MIMO with different sizes (12 mm, and 20 mm) decoupling structures.

antenna is excited, the other ports are terminated with a 50-ohm load. Similarly, the other ports of the MIMO antenna are also measured. The highest gain of the MIMO system is 6.6 dBi, which is 2 dBi higher than the single element antenna. This is due to the increase in the size of the antenna with MIMO configuration and the redistribution of the current in several radiation elements. Fig. 18 compares the values of $|S_{11}|$ that were simulated and measured. The behavior is similar in both the simulated and measured outcomes. Except for the notched band, the UWB band (3–11.8 GHz) exhibits good impedance matching.

3.1. Reflection coefficients

The arrangement of MIMO components is symmetrical in geometry; as a result, it exhibits identical reflection coefficients. The UWB tri-band-notched is proposed as a single-element antenna and the MIMO antennas' UWB bandwidth is almost identical. The measured and calculated results of the MIMO system's reflection coefficient plots are shown in Fig. 18.

3.2. Transmission coefficients

The mutual coupling between the individual elements in MIMO systems can be described as a transmission coefficient. In Fig. 19 the transmission coefficient of the final decoupling structure is depicted. Without the suggested decoupling arrangement, the antenna elements exhibit strong isolation characteristics. The UWB-MIMO antenna isolation has been reduced by the proposed

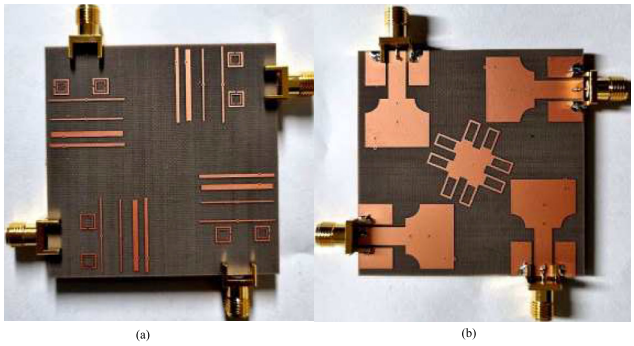

Fig. 15. Fabricated proposed UWB-MIMO antenna: (a) front-side view and (b) backside view.

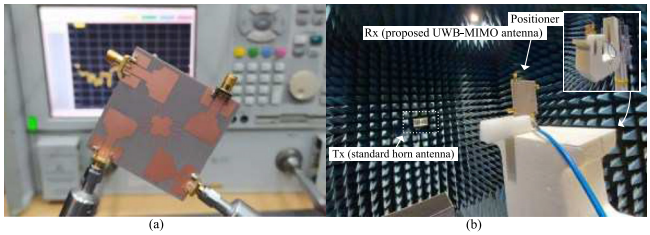

Fig. 16. Photographs of the measurements setup (a) S-parameters and (b) far-field.

novel parasitic decoupler to > 20 dB, with maximum isolation of 50 dB throughout the entire operating frequency.

3.3. Envelope correlation coefficient

The envelope correlation coefficient (ECC) is a way of measuring the correlation between the radiation patterns of the MIMO pairs. The less correlated radiation patterns are the higher the diversity gain and so the system capacity. The proposed UWB-MIMO antenna's envelope correlation coefficient is shown in Fig. 20. Ideally, this value is zero but practically less than 0.5 is applicable.

The value of the proposed MIMO system calculated ECC is less than 0.001. Equations (4) and (5) [37] can be applied to get the value of ECC of the MIMO system, transmission coefficient, and far-field radiation patterns, respectively.

$$\rho_{eij} = \frac{|S_{ii} * S_{ij} + S_{ji} * S_{jj}|^2}{(1 - |S_{ii}|^2 - S_{ij}{}^2)(1 - |S_{ji}|^2 - S_{jj}{}^2)} \tag{4}$$

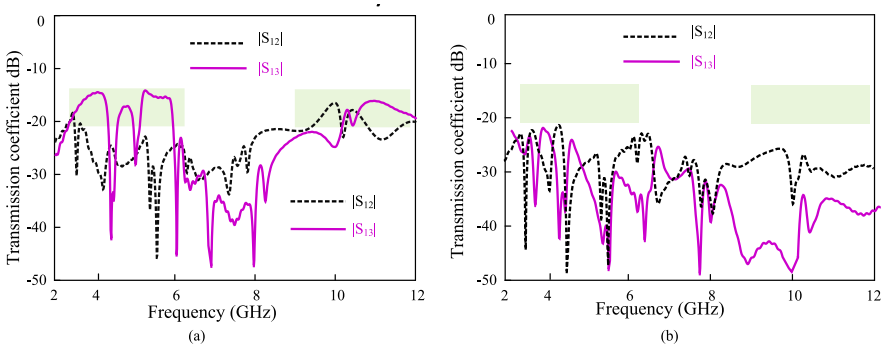

Fig. 14. The transmission coefficient of proposed UWB-MIMO (a) without and (b) with decoupling structure.

Table 3
Compared gains of the proposed UWB-MIMO antenna.

	Gain (dBi) of Antenna Element							
	Simulated values				Measured values			
	Port 1	Port 2	Port 3	Port 4	Port 1	Port 2	Port 3	Port 4
4.5	4.3	4.4	4.4	4.25	4.29	4.3	4.2	4.23
6.5	6.5	6.25	6.25	6.29	6.29	6.22	6.21	6.25
8.5	6.25	6.3	6.2	6.2	6.22	6.3	6.2	6.2
11.5	5.59	5.6	5.45	5.58	5.45	5.6	5.44	5.45

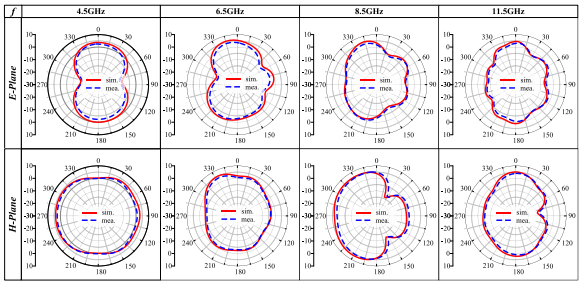

Fig. 17. The simulated E-and-H-plane radiation pattern for port-1 of the proposed UWB-MIMO antenna at 4.5, 6.5, 8.5, and 11.5 GHz frequencies.

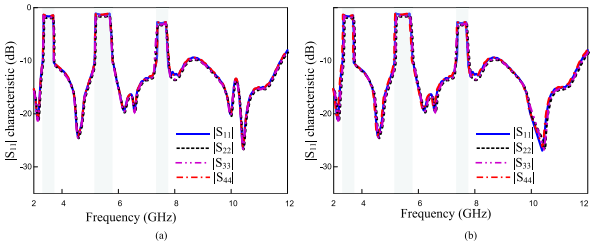

Fig. 18. |S11| characteristics of proposed UWB-MIMO antenna (a) simulated (b) measured.

$$\rho_{eij} = \frac{\left| \iint_0^{4\pi} \left[\vec{R_i}(\theta,\varphi) \times \vec{R_j}(\theta,\varphi) \right] d\Omega \right|^2}{\iint_0^{4\pi} \left| \vec{R_i}(\theta,\varphi) \right|^2 d\Omega \iint_0^{4\pi} \left| \vec{R_j}(\theta,\varphi) \right|^2 d\Omega} \tag{5}$$

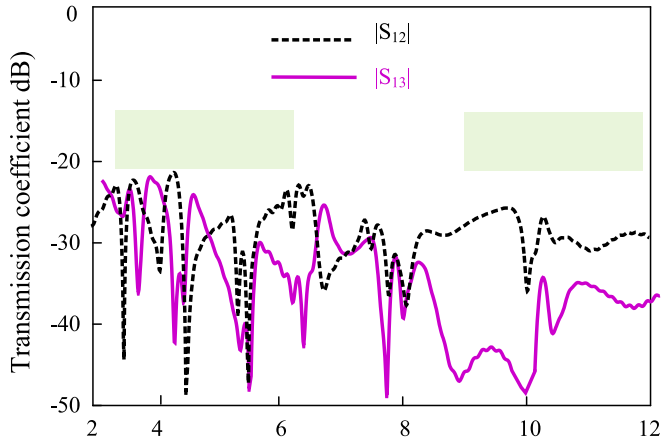

Fig. 19. The transmission coefficient of the proposed UWB-MIMO antenna.

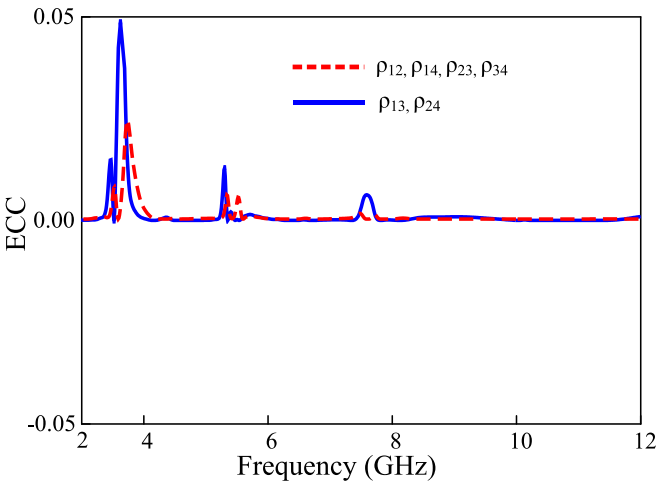

Fig. 20. The envelope correlation coefficient of the proposed antenna.

3.4. Diversity gain

Diversity gain is the increase in signal-to-noise ratio due to the diversity schemes, or the transmission power can be reduced when the diversity scheme is applied. The diversity gain of the UWB-MIMO system is demonstrated in Fig. 21, which, for all four elements other than the notched bands, is flat at the desired value of 10 dB. DG is calculated as a frequency function utilizing equation (6) [38].

$$\mathrm{DG} = 10\sqrt{1 - |\rho ij|^2} \tag{6}$$

3.5. Mean effective gain

In a multipath environment, the receiving electromagnetic power ability of the MIMO antenna is called Mean Effective Gain (MEG). It is the ratio of the mean received power to the mean incident power of the antenna. The value of MEG is shown in Fig. 22. From the figure, it can be seen that the antenna value is within the applicable MIMO system range which is less than −3 dB. This can be calculated using equation (7) [39].

$$MEGi = 0.5\left(1 - \sum_{i=1}^{N} |Sij|\right) \tag{7}$$

Where i is the port under observation and n is the antenna numbers in a MIMO system.

3.6. Channel capacity loss

In a fading environment, channel capacity refers to the data rate that is supported in a specific channel. The maximum rate at which

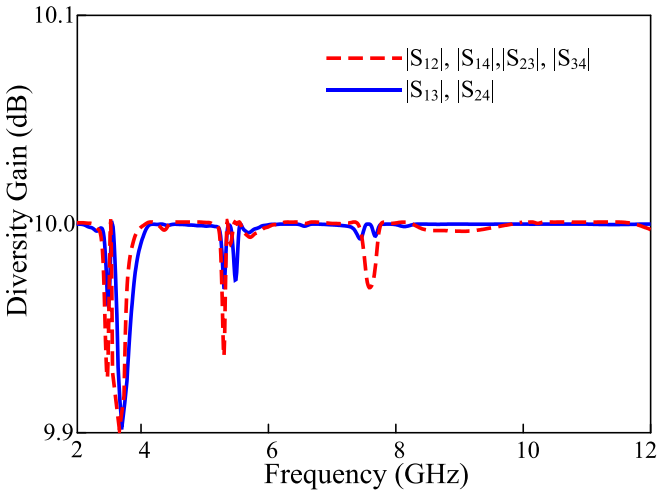

Fig. 21. Diversity Gain of the proposed antenna.

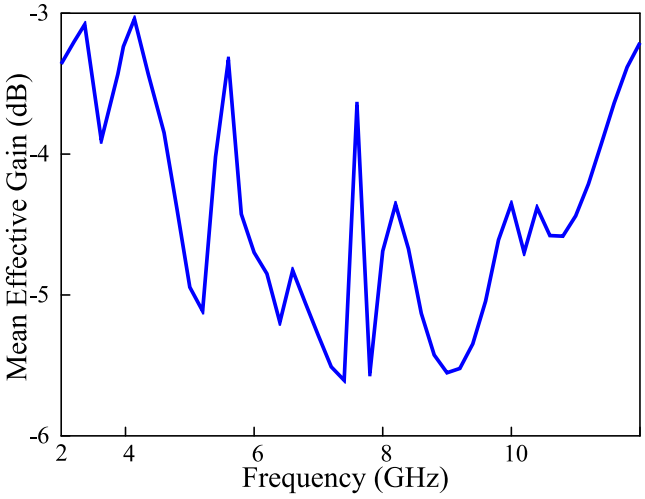

Fig. 22. Mean effective gain of the proposed antenna.

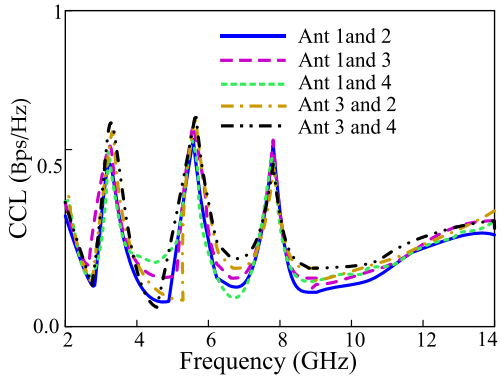

Fig. 23. CCL results of proposed UWB-MIMO antenna.

a signal can be sent across a specific MIMO antenna is known as channel capacity loss. In actual usage, CCL should not exceed 0.4 bps/Hz. To calculate capacity loss equations (8) and (9) [40,41] can be applied. The CCL of the proposed antenna is shown in Fig. 23.

$$CCL = -log_2 det|\psi^R| \tag{8}$$

where ψR Refers to the below matrix for receiving antenna correlation.

$$\psi^R = \begin{bmatrix} \rho 11 & \rho 12 & \rho 13 & \rho 14 \\ \rho 21 & \rho 22 & \rho 23 & \rho 24 \\ \rho 31 & \rho 32 & \rho 33 & \rho 34 \\ \rho 41 & \rho 42 & \rho 43 & \rho 44 \end{bmatrix} \tag{9}$$

Although our proposed MIMO antenna uses separate ground planes, it meets the requirements for MIMO performance, such as low the envelope correlation coefficient, high diversity gain and improved channel capacity.

4. Performance comparison with previous work

A performance comparison between the proposed UWB-MIMO system and the existing literature is made is depicted in Table 4. In the MIMO antenna [22], the mutual coupling among antenna elements is minimized to 15 dB by introducing a parasitic strip. In the MIMO system [24], the ground plane and parasitic resonators with reactive stub are incorporated to achieve isolation of 20 dB, however, the antenna does not have any notch to stop interference. The antenna presented in [26], has two conventional notch bands to reduce interference and the isolation of less than 15 dB is accomplished by utilizing a single structure.

Moreover, using a defective ground system technique, mutual coupling of less than 15 dB is proposed in two port UWB-MIMO antenna [27]. A quad-port UWB MIMO antenna [28] of large size offers a minimum 14.5 dB isolation, and a unique neutralization ring is created to minimize the mutual coupling effect between elements, especially for low-frequency systems by combining a rectangular ring and a straight strip line. Furthermore, the antenna does not have the advantage of band rejection of already existing bands within the UWB band. In the presented work [29], by employing a slotted stub, the isolation between the antennas is increased. The isolation of 20 dB across the entire operating range is achieved but does not have rejection bands to avoid interference. Finally, in the UWB-MIMO system [32], a large-sized 4 × 4 MIMO antenna is proposed without notching characteristics, and the authors applied metamaterial to enhance the isolation among antenna elements and able to achieve a low correlation of 15.5 dB. In summary, the proposed 2 × 2 MIMO antenna with its quasi-rectangular notch-bands prevents the potential interferences from 5G sub-GHz, WLAN, and satellite downlink bands and a good candidate for UWB applications.

5. Conclusion

In this paper, a parasitic decoupler-based UWB-MIMO antenna with three highly selective notch bands is presented. The antenna operates over the entire UWB spectrum (3.1–11.8 GHz). Already existing bands within UWB bands such as 5G Sub-6 GHz (3.4–3.8 GHz), WLAN band (5.25–5.75 GHz), and satellite downlink band (7.25–7.75 GHz) are filtered using EBG structures and SRRs. A 4-port UWB-MIMO antenna has been constructed from the single-element antenna with 14 mm space between the vertical elements. The proposed parasitic decoupling structure enhances the performance of the MIMO system, and the isolation of the antenna is improved. A good degree of consistency can be shown between the proposed antenna's measured and simulated results. The antenna offers a consistent gain with a maximum gain of 6.35 dBi, low isolation (1.2 dB enhanced compared to the simple MIMO antenna), lower ECC value (0.001), and a nearly ideal diversity gain of 9.99. The suggested antenna for the UWB-MIMO appli-

Table 4
The performance comparison of the proposed MIMO system with the published related works.

Ref	Isolation Enhancement Technique	Antenna Size (mm^2)	Notch bands	Number of Ports	ECC	Minimum isolation (dB)	Peak Gain (dBi)
[22]	Parasitic strip	34 × 34	3	4	0.05	15	5.5
[24]	Parasitic decoupler	40 × 43	0	4	0.2	20	4
[26]	Decoupling network	11.1 × 12	2	2	0.05	15	4
[27]	Defected ground	34 × 22	3	2	0.003	15	5
[28]	Neutralization lines	75.19 × 75.19	0	4	0.1	14.5	5
[29]	Slotted stubs	33 × 48	0	4	0.04	20	4.3
[32]	Metamaterials	80 × 80	0	4	0.04	15.5	8.3
This work	Parasitic decoupler	54 × 54	3	4	0.001	20	6.35

cation is stable according to the performance parameters. The suggested MIMO antenna can be used for all UWB applications, except for extremely small Internet of Things devices and rare circumstances when a UWB MIMO antennas need shared ground.

Declaration of Competing Interest

The authors declare that they have no known competing financial interests or personal relationships that could have appeared to influence the work reported in this paper.

Acknowledgments

This work was supported by the Institute of Information & Communications Technology Planning & Evaluation (IITP) grant funded by the Korean government (MSIT) (No. 2022-0-01031, Development of measured EMF big data analysis and management platform).

References

[1] M.Z. Mahmud, T. Alam, M. Samsuzzaman, A. Ullah, M.T. Islam, An Irregular Ground Oriented Miniaturized Antenna for UWB Industrial Applications, Appl. Comput. Electromagnetics Society J. (ACES) (2018) 1268–1275.
[2] K. Mekki, O. Necibi, S. Lakhdhar, A. Gharsallah, A UHF/UWB Monopole Antenna Design Process Integrated in an RFID Reader Board, J. Electromagn. Eng. Sci. 22 (4) (2022) 479–487.
[3] L. Liu, S.W. Cheung, R. Azim, M.T. Islam, A compact circular-ring antenna for ultra-wideband applications, Microw. Opt. Technol. Lett. 53 (10) (2011) 2283–2288.
[4] T. Woo, D. Kim, C.Y. Park, Y.J. Yoon, Compact Wideband Loop Antenna for Earbuds, IEEE Access 10 (2022) 47340–47347.
[5] H. Li, H. Zhang, Y. Kong, C. Zhou, Flexible Dual-Polarized UWB Antenna Sensors for Breast Tumor Detection, IEEE Sens. J. 22 (13) (2022) 13648–13658.
[6] R. Azim, M.T. Islam, N. Misran, Compact tapered-shape slot antenna for UWB applications, IEEE Antennas Wirel. Propag. Lett. 10 (2011) 1190–1193.
[7] R. Azim, M.T. Islam, N. Misran, Ground modified double-sided printed compact UWB antenna, Electron. Lett. 47 (1) (2011) 9–11.
[8] S. Ullah, C. Ruan, M.S. Sadiq, T.U. Haq, W. He, High efficient and ultra-wide band monopole antenna for microwave imaging and communication applications, Sensors 20 (1) (2019) 115.
[9] J. Logeswaran, R.B. Rani, UWB Antenna as a Sensor for the Analysis of Dissolved Particles and Water Quality, Progress Electromagnetics Res. Letters 106 (2022) 31–39.
[10] M.T. Islam, R. Azim, A.T. Mobashsher, Triple band notched planar UWB antenna using parasitic strips, Prog. Electromagn. Res. 129 (2012) 161–179.
[11] N. Hussain, M. Jeong, J. Park, S. Rhee, P. Kim, N. Kim, A compact size 2.9-23.5 GHz microstrip patch antenna with WLAN band-rejection, Microwave and Optical Tech. Lett. 61 (5) (2019) 1307–1313.
[12] C. Ramakrishna, G.A.E. Kumar, P.C.R. Sekhar, Quadruple Band-Notched Compact Monopole UWB Antenna for Wireless Applications, J. Electromagnet Eng. Sci. 21 (5) (2021) 406–416.
[13] A. Abbas, N. Hussain, M.J. Jeong, J. Park, K.S. Shin, T. Kim, N. Kim, A rectangular notch-band UWB antenna with controllable notched bandwidth and centre frequency, Sensors 20 (3) (2020) 777.
[14] A. Abbas, N. Hussain, J. Lee, S.G. Park, N. Kim, Triple rectangular notch UWB antenna using EBG and SRR, IEEE Access 9 (2021) 2508–2515.
[15] F. Zhu, S. Gao, A.T. Ho, R.A. Abd-Alhameed, C.H. See, T.W. Brown, J. Xu, Multiple band-notched UWB antenna with band-rejected elements integrated in the feed line, IEEE Trans. Antennas Propag. 61 (8) (2013) 3952–3960.
[16] F. Jaglan, S.D. Gupta, E. Thakur, D. Kumar, B.K. Kanaujia, S. Srivastava, Triple band notched mushroom and uniplanar EBG structures based UWB MIMO/Diversity antenna with enhanced wide band isolation, AEU-Int. J. Electron. Commun. 90 (2018) 36–44.
[17] N. Jaglan, S.D. Gupta, B.K. Kanaujia, M.S. Sharawi, 10 element sub-6-GHz multi-band double-T based MIMO antenna system for 5G smartphones, IEEE Access 9 (2021) 118662–118672.
[18] D. Potti, Y. Tusharika, M.G.N. Alsath, S. Kirubaveni, M. Kanagasabai, R. Sankararajan, P.B. Bhargav, A novel optically transparent UWB antenna for automotive MIMO communications, IEEE Trans. Antennas and Propag. 69 (7) (2021) 3821–3828.
[19] Z. Tang, J. Zhan, X. Wu, Z. Xi, S. Wu, Simple ultra-wider-bandwidth MIMO antenna integrated by double decoupling branches and square-ring ground structure, Microw. Opt. Technol. Lett. 62 (3) (2020) 1259–1266.
[20] M.A. Sufian, N. Hussain, A. Abbas, J. Lee, S.G. Park, N. Kim, Mutual Coupling Reduction of a Circularly Polarized MIMO Antenna Using Parasitic Elements and DGS for V2X Communications, IEEE Access 10 (2022) 56388–56400.
[21] M.A. Sufian, N. Hussain, H. Askari, S.G. Park, K.S. Shin, N. Kim, Isolation enhancements of a metasurface-based MIMO antenna using slots and shorting pins, IEEE Access 9 (2021) 73533–73543.
[22] Z. Tang, X. Wu, J. Zhan, S. Hu, Z. Xi, Y. Liu, Compact UWB-MIMO Antenna with High Isolation and Triple Band-Notched Characteristics, IEEE Access 7 (2019) 19856–19865.
[23] M.M. Hassan, M. Rasool, M.U. Asghar, Z. Zahid, A.A. Khan, I. Rashid, A. Rauf, F.A. Bhatti, A novel UWB MIMO antenna array with band notch characteristics using parasitic decoupler, J. Electromagnet. Waves Appl. 34 (9) (2020) 1225–1238.
[24] F. Amin, R. Saleem, T. Shabbir, S.U. Rehman, M. Bilal, M.F. Shafique, A compact quad-element UWB-MIMO antenna system with parasitic decoupling mechanism, Appl. Sci. 9 (11) (2019) 2371.
[25] A. Abbas, N. Hussain, M.A. Sufian, J. Jung, S.M. Park, N. Kim, Isolation and Gain Improvement of a Rectangular Notch UWB-MIMO Antenna, Sensors 22 (4) (2022) 1460.
[26] T.C. Tang, K.H. Lin, An ultrawideband MIMO antenna with dual band-notched function, IEEE Antennas Wirel. Propag. Lett. 13 (2014) 1076–1079.
[27] K. Patchala, Y. Raja Rao, A.M. Prasad, Triple band notch compact MIMO antenna with defected ground structure and split ring resonator for wideband applications, Heliyon 6 (1) (2020) e03078.
[28] A. Kayabasi, A. Toktas, E. Yigit, K. Sabanci, Triangular quad-port multi-polarized UWB MIMO antenna with enhanced isolation using neutralization ring, AEU- Int. J. Electron. Commun. 85 (2018) 47–53.
[29] A. Altaf, A. Iqbal, A. Smida, J. Smida, A.A. Althuwayb, S. Hassan Kiani, M. Alibakhshikenari, F. Falcone, E. Limiti, Isolation improvement in UWB-MIMO antenna system using slotted stub, Electronics 9 (10) (2020) 1582.
[30] G. Saxena, Y.K. Awasthi, P. Jain, Design of metasurface absorber for low RCS and high isolation MIMO antenna for radio location & navigation, AEU- Int. J. Electron. Commun. 133 (2021) 153680.
[31] A.H. Jabire, A. Ghaffar, X.J. Li, A. Abdu, S. Saminu, M. Alibakhshikenari, F. Falcone, E. Limiti, Metamaterial based design of compact UWB/MIMO monopoles antenna with characteristic mode analysis, Appl. Sci. 11 (4) (2021) 1542.
[32] M. Hasan, M.T. Islam, M. Samsuzzaman, M.H. Baharuddin, M.S. Soliman, A. Alzamil, M. Islam, Gain, and isolation enhancement of a wideband MIMO antenna using metasurface for 5G sub-6 GHz communication systems, Sci. Rep. 12 (1) (2022) 1–17.
[33] C. Valagiannopoulos, T.A. Tsiftsis, V. Kovanis, Metasurface-enabled interference mitigation in visible light communication architectures, J. Opt. 21 (11) (2019) 11570.
[34] Y. Li, H. Yang, H. Cheng, J. Wu, Y. Yang, L. Hua, Y. Wang, Isolation enhancement in dual-band MIMO antenna by using metamaterial and slot structures for WLAN applications, J. Phys. D Appl. Phys. 55 (32) (2022) 325103.
[35] Y. Feng, Z. Li, L. Qi, W. Shen, G. Li, A compact and miniaturized implantable antenna for ISM band in wireless cardiac pacemaker system, Sci. Rep. 12 (1) (2022) 1–11.
[36] T. Govindan, S.K. Palaniswamy, M. Kanagasabai, T.R. Rao, M.G.N. Alsath, S. Kumar, S. Velan, M. Marey, A. Aggarwal, On the design and performance analysis of wristband MIMO/diversity antenna for smart wearable communication applications, Sci. Rep. 11 (1) (2021).
[37] H.T. Hui, Decoupling methods for the mutual coupling effect in antenna arrays: a review, Recent Patents Eng. 1 (2) (2007) 187–193.

[38] K. Muhammad Irshad, K. Muhammad Irfan, M. Al-Hassan, Miniaturized MIMO antenna with low inter-radiator transmittance and band rejection features, J. Electromagn Eng. Sci. 21 (4) (2021) 307–315.
[39] M.D. Alanazi, S.K. Khamas, A Compact Dual Band MIMO Dielectric Resonator Antenna with Improved Performance for mm-Wave Applications, Sensors 22 (13) (2022) 5056.
[40] S. Ahmad, S. Khan, B. Manzoor, M. Soruri, M. Alibakhshikenari, M. Dalarsson, F. Falcone, A compact CPW-fed ultra-wideband multi-input-multi-output (MIMO) antenna for wireless communication networks. IEEE, Access 10 (2022) 25278–25289.
[41] A. Khan, S. Bashir, S. Ghafoor, K.K. Qureshi, Mutual coupling reduction using ground stub and EBG in a compact wideband MIMO-antenna, IEEE Access 9 (2021) 40972–40979.